ISSN 1070-3284, Russian Journal of Coordination Chemistry, 2019, Vol. 45, No. 5, pp. 361–370. © Pleiades Publishing, Ltd., 2019.
Russian Text © The Author(s), 2019, published in Koordinatsionnaya Khimiya, 2019, Vol. 45, No. 5, pp. 311–320.

Yttrium Coordination Compounds with Nitrilotris(Methylenephosphonic Acid)

N. V. Somov[a, *], F. F. Chausov[b, c], N. V. Lomova[b], R. M. Zakirova[c], V. G. Petrov[b], D. K. Zhirov[b], and M. A. Shumilova[b]

[a] *Lobachevsky State University of Nizhny Novgorod, Nizhny Novgorod, 603950 Russia*
[b] *Udmurt Federal Research Center, Ural Branch, Russian Academy of Sciences, Izhevsk, 426067 Russia*
[c] *Udmurt State University, Izhevsk, 426034 Russia*
**e-mail: somov@phys.unn.ru*

Received June 8, 2018; revised August 16, 2018; accepted December 24, 2018

Abstract—Nitrilotris(methylenephosphonato)yttrium $[YH_3\{N(CH_2PO_3)_3\}] \cdot 2H_2O$ (**I**) and octapotassium monohydro-bis-nitrilotris(methylenephosphonato)yttriate pentadecahydrate $K_8[YH\{N(CH_2PO_3)_3\}_2] \cdot 15H_2O$ (**II**) were synthesized and studied. The structure of **II** was determined by X-ray diffraction (CIF file CCDC no. 1847628). The crystals of **II** are triclinic, space group $P\bar{1}$, $Z = 2$, $a = 11.0264(8)$, $b = 11.3857(8)$, $c = 16.6938(6)$ Å, $\alpha = 86.455(4)°$, $\beta = 85.269(4)°$, $\gamma = 85.319(6)°$. The ligand molecules are crystallographically and functionally non-equivalent; one is completely deprotonated and chelates the Y atom via one N- and three O-donor centers and the other one chelates the Y atom via two O atoms.

Keywords: yttrium, coordination compounds, nitrilotris(methylenephosphonates), chelate complexes, crystal structure, X-ray photoelectron spectra

DOI: 10.1134/S1070328419030096

INTRODUCTION

Yttrium ($[Kr]5s^24d^1$) is often considered as a chemical analogue of lanthanides, especially heavy lanthanides [1–3].

In cancer therapy, coordination compounds of ^{90}Y, which is a β^--emitter free from accompanying γ-radiation, are used for the radiation therapy of bone metastases [4, 5]. The selective binding of Y complexes in the body provides targeted drug delivery and reduces the radiation exposure of healthy tissue.

In metallurgy, Y present in 0.5–1.5% concentrations markedly enhances the heat resistance and decreases the rates of gas and plasma corrosion of chromium steels [6, 7] and other refractory alloys [8, 9]. This is due to surface segregation of yttrium [10, 11] and formation of a layer consisting of very stable Y_2O_3 ($\Delta H^0_{f298} = -1903$ kJ/mol [12]) and mixed oxides, strongly attached to the metal surface. High cost and deficiency of yttrium stimulates the interest in the development of surface doping of steel articles: electroexplosive deposition [13, 14], laser treatment [15], and ion implantation [16]. All these methods have some drawbacks, which include coating non-uniformity, crack formation, and disruption of the metal structure. A method has been proposed for steel surface modification by thermal conversion of the adsorbed layer of an Y-containing precursor [17]. It may be expected that yttrium coordination compounds with promiscuous ligands able to form coordination bonds with many elements of the alloy surface layer would be the most promising precursors for fabrication of a homogeneous Y-containing adsorption layer. Therefore, yttrium coordination chemistry is a relevant investigation subject.

Yttrium bears resemblance to both typical *d*-elements of periods 4 and 5 and lanthanides and, hence, it has a diversified coordination chemistry and a broad range of coordination numbers (CNs). For example, in the complexes with pyridine-2,6-dicarboxylic [18] and oxalic acids [19], yttrium has CN 9 and a distorted tricapped trigonal prism geometry. In the binuclear complex of quinolne-4-carboxylic acid [20], the Y atom is coordinated by nine O atoms (including two water molecules) in a distorted monocapped square antiprism; this discloses group analogy between Y and lanthanum and lanthanides. Conversely, when complexed with propionate ligands, yttrium resembles analogues of periods 4 and 5. For example, in the *N*,*N*'-2-methylpiperazine-bis(methylenephosphonic acid) complex [21], the CN(Y) is six and the coordination polyhedron (CP) is close to a trigonal antiprism. When Y is coordinated by (1,1'-biphenyl)-3,3',5,5'-tetrakis-phosphonic acid [22], the yttrium CP is a slightly distorted octahedron. Apparently, this is due

to a larger size and steric rigidity of phosphonate ligands as compared with carboxylate ones.

In recent years, N,O-ligands such as aminopolyphosphonic acids, in particular, nitrilotris(methylenephosphonic acid) ($N(CH_2PO_3)H_6$, NTP) have received considerable attention both in Russia and abroad. Coordination compounds of NTP with many metals [23–32], including lanthanum [32], have been investigated. The stepwise deprotonation of O- and N-donor centers of NTP provides efficient control over the structure and properties of the obtained complexes [33, 34] and surface layers they form upon adsorption [35–37]. However, the structure of Y complexes with NTP has not been studied.

A study of the stability constants of NTP complexes of Sc and Y has shown [38] that the first protonation constant of the complex (pK_{MHL}) depends on the ionic radius of the complexing metal and is determined by the competition between proton and the metal ion for the N-donor center, while the second (pK_{MH2L}) and subsequent constants do not depend on the metal nature and are associated with the protonation of free O-donor centers. For Y complexes with NTP, the first constant $pK_{MHL} = 7.15 \pm 0.02$ and the second one $pK_{MH2L} = 5.5 \pm 0.06$; this gap attests to high basicity of the N-donor center. The large difference from the protonation constants of the free ligand ($pK_{HL} = 12.7 \pm 0.1$, $pK_{H2L} = 7.15 \pm 0.02$) is indicative of a considerable Y^{3+} affinity for the NTP donor centers.

This publication describes the synthesis, structure, and some properties of octapotassium monohydrobis-nitrilotris(methylenephosphonato)yttriate pentadecahydrate $K_8[YH\{N(CH_2PO_3)_3\}_2] \cdot 15H_2O$ (**II**).

EXPERIMENTAL

Synthesis of $[YH_3\{N(CH_2PO_3)_3\}] \cdot 2H_2O$ (I). A solution of reagent grade $Y(NO_3)_3 \cdot 6H_2O$ (3.83 g, 0.01 mol) was added dropwise at 70–90°C to an aqueous solution of NTP (twice crystallized) (3.3 g, 0.011 mol). The mixture was stirred for 1 h at 70–90°C, and the precipitate of **I** was separated on a filter, washed with distilled water to neutral pH, and dried in a desiccator to a constant weight. The yield of **I** was 3.96 g (94%). Quantitative analysis was carried out according to the State Standard GOST 10398-76 (Y) and Federal Nature Protective Regulatory Document PND F 14.1:4.248-07 (P).

For $C_3H_{13}NO_{11}P_3Y$ (**I**)

Anal calcd., %	Y, 21.12	P, 22.07
Found, %	Y, 20.4 ± 0.5	P, 22.5 ± 0.5

Synthesis of $K_8[YH\{N(CH_2PO_3)_3\}_2] \cdot 15H_2O$ (II). Compound **I** (3.85 g, 0.01 mol) was added to an aqueous solution of NTP (2.99 g, 0.01 mol) and reagent grade KOH (5.21 g, 0.08 mol). The reaction mixture (pH 7.8 ± 0.2) was stirred for 1 h at 60–80°C and filtered. DMSO (1/3 by volume) was added, and the mixture was stirred and crystallized under isothermal conditions under slow solvent evaporation. The crystals of **II** were colorless columnar prisms. The yield of **II** was 9.32 g (74%).

For $C_6H_{43}N_2O_{33}P_6K_8Y$ (**II**)

Anal calcd., %	Y, 7.06	P, 14.76
Found, %	Y, 7.2 ± 0.5	P, 14.2 ± 0.5

X-ray diffraction. The primary structural fragments were found by the direct method and the atomic positions were derived from the difference electron density maps. The non-hydrogen atom parameters were refined in the anisotropic approximation by the least squares method on $|F|^2$. The hydrogen atom positions for the ligand were refined in the isotropic approximation. The positions of hydrogen atoms of the water molecules could not be located from X-ray diffraction data. Crystallographic data and X-ray experiment and structure refinement details for **II** are summarized in Table 1. Selected interatomic distances and bond and torsion angles for **II** are given in Table 2.

The X-ray diffraction data are deposited with the Cambridge Crystallographic Data Centre (CCDC no. 1847628; deposit@ccdc.cam.ac.uk or http://www.ccdc.cam.ac.uk).

The X-ray photoelectron spectra (XPS) of **I** and **II** were measured on an EMS-3 X-ray electron spectrometer (Udmurt Federal Research Center, UB RAS, Russia) [44] with a magnetic energy analyzer with AlK_α excitation ($h\nu = 1486.6$ eV). The finely powdered samples were deposited on a pyrolytic graphite substrate as 1–3 μm-thick layers. During recording of the spectra, the samples were heated *in situ* (in the working space of the spectrometer) from room temperature to 400°C, with the gaseous products of destruction being continuously pumped out. The residual pressure in the working space did not exceed 10^{-5} Pa. The energy analyzer was calibrated against the C1*s* spectrum (binding energy $E_b = 284.5$ eV). The P2*p*, Y3*d*, N1*s*, and valence band spectra were recorded. The background and inelastic scattering corrections were applied according to Shirley [45]. The statistical processing of experimental data was performed using the Fityk 0.9.8 software [46].

The IR spectra of **I**, **II**, and thermal decomposition products were measured in KBr pellets (test compound, 1 mg; KBr, 250 mg) on an FSM-1201 FT IR spectrometer in the 450–5000 cm^{-1} range. The Raman spectra of **I** and **II** were measured on a Centaur U-HR microscope microspectrometer in the 475–575 nm range (laser excitation at $\lambda = 473$ nm). Thermogravimetric analysis of **I** and **II** was carried out on a Shimadzu DTG-60H automated derivatograph in

Table 1. Crystallographic data and X-ray diffraction experiment and structure refinement details for compound **II**

Parameter	Value
Molecular formula	$C_6H_{43}N_2O_{33}P_6K_8Y$
M	1258.93
System; space group; Z	Triclinic; $P\bar{1}$; 2
a, Å	11.0264(8)
b, Å	11.3857(8)
c, Å	16.6938(6)
α, deg	86.455(4)
β, deg	85.269(4)
γ, deg	85.319(6)
V, Å^3	2078.5(2)
ρ(calcd.), g/cm^3	1.963
Radiation; λ, Å	MoK_α; 0.71073
μ, mm^{-1}	2.535
T, K	100(2)
Crystal size, mm	0.179 × 0.109 × 0.058
Diffractometer	XtaLAB Pro MM003, PILATUS 200K
Scan mode	ω
Absorption correction	Analytic [39]
T_{min}/T_{max}	0.664/0.88
$\theta_{min}/\theta_{max}$, deg	1.797/26.372
Ranges of h, k, l	$-13 \le h \le 13$, $-14 \le k \le 14$, $-20 \le l \le 20$
Number of measured/unique reflections (N_1)	34366/8483
R_{int}	0.0716
Number of reflections with $I > 2\sigma(I)$ (N_2)	6835
Method of refinement	Full-matrix least-squares on F^2
Number of parameters/restraints	534/0
S	1.215
R_1/wR_1 for N_1	0.1053/0.2103
R_1/wR_1 for N_2	0.0864/0.2035
$\Delta\rho_{min}/\Delta\rho_{max}$, e/Å^3	−1.014/0.184
Software	CrysAlisPro [40], SHELX-2014 [41], WinGX [42], VESTA 3.0 [43]

the 30–500°C temperature range at a heating rate of 3°C/min under argon.

RESULTS AND DISCUSSION

The structure of the inner coordination sphere of complex **II** is shown in Fig. 1a. Yttrium is coordinated by two NTP molecules, one of them being completely deprotonated. It coordinates the Y(1) atom via N(1) atom and three O atoms (one from each PO_3 group) and also coordinates the Y(1)* atom via two O atoms of the complex formula unit symmetrically equivalent relative to the inversion center. This gives rise to three five-membered intramolecular rings Y–N–C–P–O sharing the Y–N bond and an eight-membered intermolecular ring Y–O–P–O–Y–O–P–O. Complete deprotonation of this NTP molecule is indicated by the P–O distances (1.504(9)–1.537(9) Å; average, 1.523(11) Å), in particular, the P–O bond is elongated upon the protonation to 1.55–1.56 Å [27–29, 31–33]. The P–O distances are longer by 0.021 Å for the yttrium-coordinated O atoms (1.533(8)–1.537(9) Å; average, 1.534(2) Å) than for the O atoms not involved in Y coordination (1.504(9)–1.522(8) Å; average,

Table 2. Selected interatomic distances (*d*) and bond (ω) and torsion (φ) angles in structure **II**

Bond	*d*, Å	Bond	*d*, Å	Bond	*d*, Å
Y(1)–N(1)	2.672(9)	C(1)–P(1)	1.816(11)	P(3)–O(8)	1.514(8)
Y(1)–O(1)	2.234(8)	C(2)–P(2)	1.822(11)	P(3)–O(9)	1.504(9)
Y(1)–O(4)	2.287(8)	C(3)–P(3)	1.809(10)	P(4)–O(10)^{Y}	1.513(8)
Y(1)–O(7)	2.295(8)	C(4)–P(4)	1.813(12)	P(4)–O(11)	1.518(8)
Y(1)–O(3)*	2.262(7)	C(5)–P(5)	1.844(12)	P(4)–O(12)	1.518(9)
Y(1)–O(10)	2.266(8)	C(6)–P(6)	1.829(11)	P(5)–O(13)^{Y}	1.528(8)
Y(1)–O(13)	2.322(8)	P(1)–O(1)^{Y}	1.535(8)	P(5)–O(14)	1.509(10)
N(1)–C(1)	1.465(13)	P(1)–O(2)	1.512(8)	P(5)–O(15)	1.521(10)
N(1)–C(2)	1.484(13)	P(1)–O(3)^{Y}	1.533(8)	P(6)–O(16)	1.500(9)
N(1)–C(3)	1.472(14)	P(2)–O(4)^{Y}	1.537(9)	P(6)–O(17)	1.521(9)
N(2)–C(4)	1.516(15)	P(2)–O(5)	1.522(8)	P(6)–O(18)	1.515(10)
N(2)–C(5)	1.490(14)	P(2)–O(6)	1.516(8)	N(2)–H	0.981(9)
N(2)–C(6)	1.510(15)	P(3)–O(7)^{Y}	1.533(8)	N(2)–O(7)	2.688(12)
K(1)–O	2.672(9)–3.250(8)	K(4)–O	2.636(9)–3.329(11)	K(7)–O	2.744(10)–3.06(4)
K(2)–O	2.613(8)–3.442(8)	K(5)–O	2.662(11)–2.856(9)	K(8)–O	2.631(14)–3.183(9)
K(3)–O	2.610(12)–3.195(16)	K(6)–O	2.717(9)–3.257(9)		
Angle	ω, deg	Angle	ω, deg	Angle	ω, deg
N(1)Y(1)O(1)	70.23(16)	O(10)Y(1)O(13)	81.40(17)	HN(2)C	105.4(5)
N(1)Y(1)O(4)	69.27(16)	O(13)Y(1)O(3)*	84.94(17)	C(4)N(2)C(5)	113.4(5)
N(1)Y(1)O(7)	68.80(15)	O(1)Y(1)O(3)*	85.88(17)	C(5)N(2)C(6)	113.7(5)
N(1)Y(1)O(3)*	132.43(16)	O(4)Y(1)O(10)	84.28(17)	C(6)N(2)C(4)	112.5(5)
N(1)Y(1)O(10)	129.47(17)	O(7)Y(1)O(13)	79.28(16)	N(1)C(1)P(1)	113.2(4)
N(1)Y(1)O(13)	129.90(17)	Y(1)N(1)C(1)	106.5(3)	N(1)C(2)P(2)	111.1(4)
O(1)Y(1)O(4)	106.90(17)	Y(1)N(1)C(2)	107.9(4)	N(1)C(3)P(3)	113.0(4)
O(4)Y(1)O(7)	111.77(17)	Y(1)N(1)C(3)	109.0(3)	N(2)C(4)P(4)	113.4(4)
O(7)Y(1)O(1)	106.27(18)	C(1)N(1)C(2)	110.4(4)	N(2)C(5)P(5)	115.2(4)
O(3)*Y(1)O(10)	80.04(17)	C(2)N(1)C(3)	111.3(4)	N(2)C(6)P(6)	120.0(4)
		C(3)N(1)C(1)	111.4(5)	N(2)HO(7)	154.4(4)
Angle	φ, deg	Angle	φ, deg	Angle	φ, deg
N(1)C(1)P(1)O(1)	31.59(10)	N(1)C(3)P(3)O(7)	33.57(10)	N(2)C(5)P(5)O(13)	41.61(11)
N(1)C(2)P(2)O(4)	34.70(10)	N(2)C(4)P(4)O(10)	51.42(10)		

* Symmetrically equivalent position: $-x, -y, -z$.
^{Y} Oxygen atom coordinating yttrium.

1.513(6) Å). This means that the electron density shifts from the P–O to Y–O bond; hence, the latter bond has a considerable covalent component. The formation of the Y–N coordination bond is indicated by the bond angles at the N(1) atom (106.5(3)°–111.4(5)°; average, 109.4(18)°) that are close to the tetrahedral angle (109.47°). Thus, this ligand molecule is pentadentate and performs both chelating and bridging coordination of Y atoms; its conformation is nearly trigonal-pseudosymmetric, which is manifested as similar interatomic distances and bond and torsion angles between atoms of the three N–C–P branches of the molecule. The dihedral angles between the N(1)Y(1)C planes are 118.58(13)°–121.07(13)° (average, 120.0(7)°).

The second NTP molecule is bidentate; it coordinates the Y(1) atom via two O atoms of two PO_3 groups, thus closing an eight-membered chelate ring Y–O–P–C–N–C–P–O. The third PO_3 group of this NTP molecule is not involved in Y coordination. The nitrogen atom of this NTP molecule is protonated and forms an H-bond with the O(7) atom of the first ligand molecule. All O atoms of this ligand molecule are deprotonated, which is confirmed by analysis of P–O distances (1.500(9)–1.528(8) Å; average, 1.516(8) Å). The P–O distances are 1.513(8) and 1.528(8) Å (average, 1.521(8) Å) for the O atoms involved in Y coordination and 1.500(9)–1.521(10) Å (average, 1.515(7) Å) for the free O atoms. The conformation of this ligand molecule is fully asymmetrical, which is manifested as a sharp difference between interatomic distances and bond and torsion angles between atoms of its N–C–P branches.

Thus, the two NTP molecules incorporated in the inner coordination sphere of complex **II** are nonequivalent in the crystallographic position, chemical function, and the acid-base state. This sharply distinguishes complex **II** from the NTP complex of La [32], in which two ligand molecules are arranged symmetrically in the coordination sphere, are both completely deprotonated, and chelate the La atoms with CN(La) being eight. Apparently, this NTP behavior in yttrium complex **II** is attributable to specific complex-forming properties of yttrium. In complex **II**, the CN(Y) is 7, which is typical of many period 5 elements. The yttrium CP is a distorted trigonal antiprism, with the vertices being occupied by O atoms and the capping vertex above the base being occupied by an additional nitrogen atom. The Y–O distances are 2.234(8)–2.322(8) Å (average, 2.278(21) Å), which is 0.28(4) Å shorter than the expected sum of the Y and O covalent radii of 2.56 Å [47] (r(Y) = 1.90(7), r(O) = 0.66(2) Å). This is probably due to considerable donation of the oxygen electron density to the Y–O bonds. The Y–N distance in **II** (2.672(9) Å) is, conversely, longer by 0.06(4) Å than the sum of the Y and N covalent radii of 2.61 Å (r(N) = 0.71(1) Å), which is attributable to relatively weak electron-donor properties of nitrogen. Apparently, the Y covalent radius, which is much shorter than r(La) (2.07(8) Å), and the steric rigidity of the pentadentate NTP ligand prevent the CN(Y) from increasing to eight. The competition between the O- and N-donor centers of the second NTP molecule for yttrium precludes the Y coordination by the second N atom. Thus, different acid-base states of two ligand molecules in complex **II** are due to stereochemical features of Y coordination.

The crystal packing of complex **II** is shown in Fig. 1b. The formula unit of the complex is asymmetrical; the $P\bar{1}$ symmetry group of the crystal packing is caused by symmetrical positions of the formula units relative to the inversion centers (Fig. 1b conventionally shows only one formula unit). The complex anions $[YH\{N(CH_2PO_3)_3\}_2]^{8-}$, which are symmetrically positioned in adjacent lattice cells, are connected in pairs by O–Y coordination bonds (Fig. 1a). The crystal structure is of the island type; the complex anions $[YH\{N(CH_2PO_3)_3\}_2]^{8-}$ are surrounded by the potassium hydrate cations, thus forming a continuous 3D interwoven network of K^+–$(H_2O)_n$ cations. The positions of two potassium ions (K(7) and K(8)) are disordered. The water molecules coordinating them are also disordered, which accounts for the apparent short K–O(w) contacts. Actually, when each site is populated by K^+ ions, water molecules occupy only the sterically suitable positions of the coordination sphere. Also, water molecules are hydrogen-bonded to one another and to oxygen atoms of the NTP PO_3 groups; however, pronounced disorder of the water molecules precluded location of most hydrogen atoms and hydrogen bonds.

The XPS of complexes **I** and **II** are shown in Fig. 2. The P2p spectrum of compound **I** (Fig. 2, *1*) comprises two components with the width at half height (WHH) of 2 eV. According to published data [31, 37, 48], the low-energy component (E_b = 132.2 eV) refers to the PO_3 groups that coordinate the metal atom, while the high-energy component (E_b = 133.9 eV) belongs to free PO_3 groups. The integrated intensity ratio of 2 : 1 suggests that in structure **I**, two PO_3 groups are coordinated to the Y atom, while one group is not involved in the coordination. The Y3d spectrum of complex **I** is a spin–orbit doublet with E_b = 154.7 and 157.5 eV, the WHH of each component is 2 eV and the integrated intensity ratio is 3 : 2. The N1s spectrum of compound **I** has only one component with WHH of 2.12 eV and a maximum at E_b = 400.8 eV, which is typical of nitrogen in the R_3N^+–H environment [49, 50]. The valence band spectrum (Fig. 2b) shows occupied molecular states with E_b ~ 5, 7, and 10 eV and localized P3s, O2s, Y4p, and Y4s electron states.

In the XPS of compound **II** (Fig. 2, *2*), the integrated intensity ratio of P2p components with E_b of 132.2 and 134.7 eV is ~5 : 1, which allows E_b = 132.2 eV to be assigned to the P(1)–P(5) atoms and E_b =

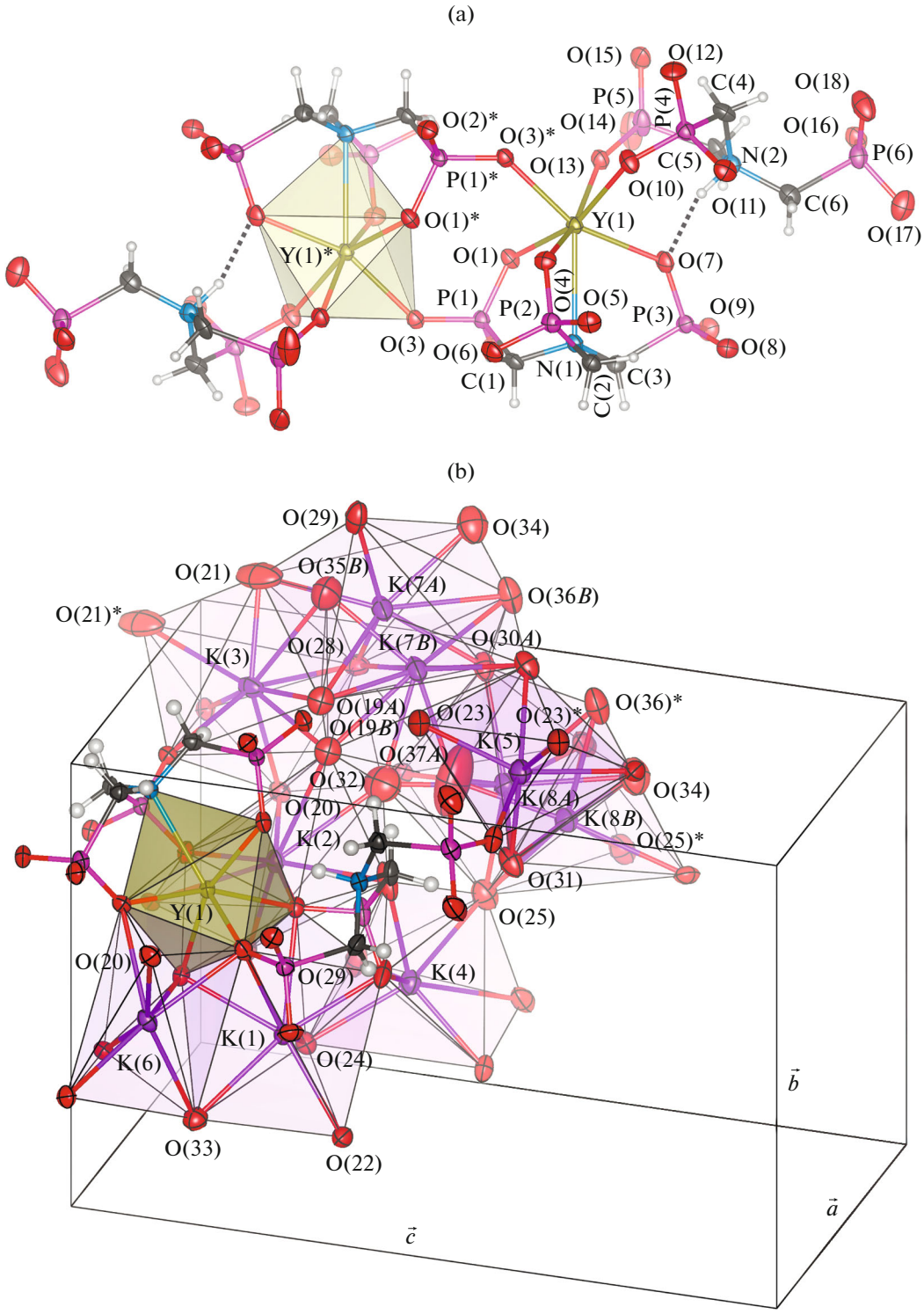

Fig. 1. (a) Inner coordination sphere of complex **II**, (b) crystal packing of complex **II** in the Y (dark) and K (light) coordination polyhedra (only one of symmetrically located formula units is shown); * are symmetrically equivalent positions.

134.7 eV to be assigned to P(6). The Y3*d* spin–orbit doublet includes components with E_b = 153.9 and 156.6 eV and WHH 3 eV. The decrease in the E_b of Y3*d* by 0.8–0.9 eV in comparison with complex **I** is attributable to the back donation of the oxygen electron density to Y. The N1*s* spectrum of compound **II** has

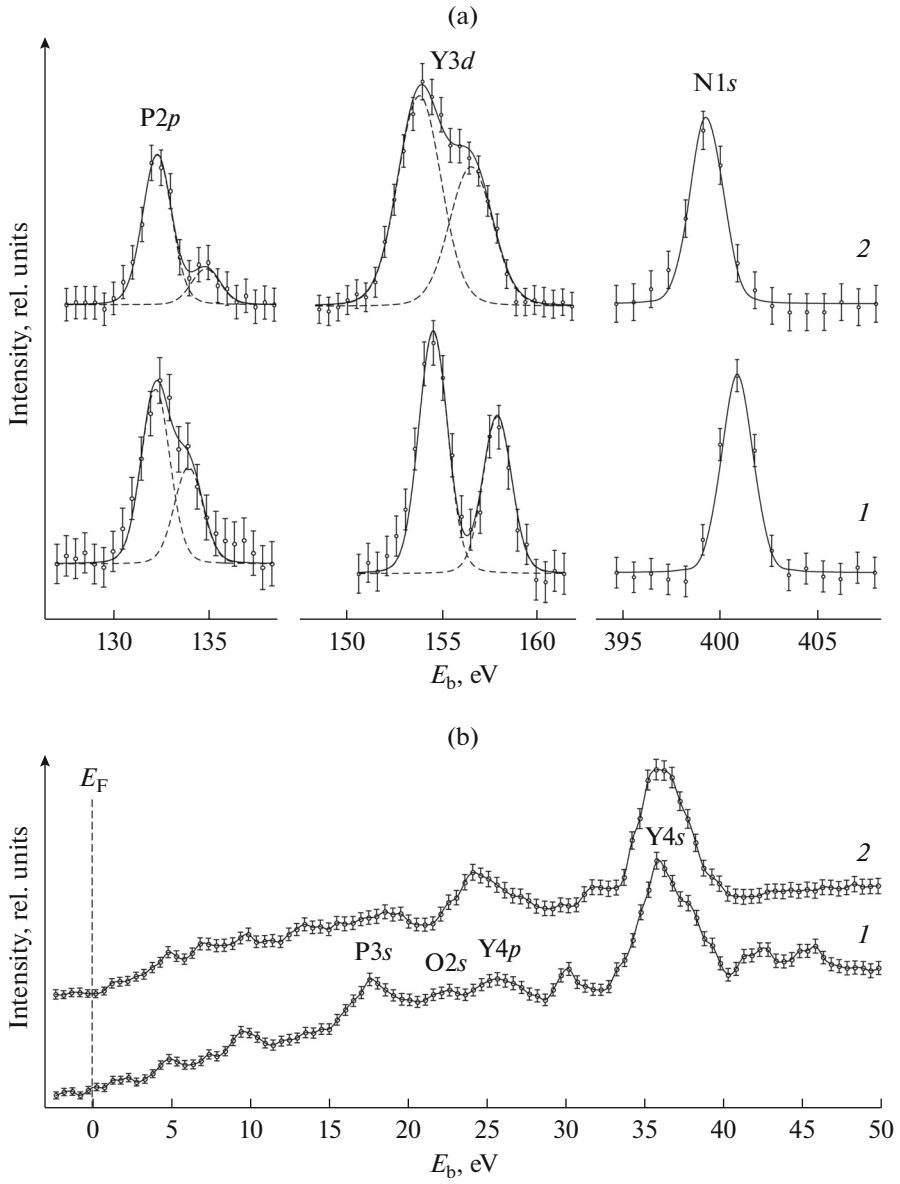

Fig. 2. XPS of (a) inner levels and (b) weakly bound electrons of complexes (*1*) **I** and (*2*) **II**. Intensity vs. binding energy E_b, the bars show 95% confidential intervals for the intensity.

WHH of 2.2 eV and E_b = 399.2 eV, which is similar to N1*s* binding energy in nitrides [51–53] and confirms the formation of the Y–N coordination bond. In the valence band spectrum, the intensity peaks of the P3*s* states approach each other and the electron density at the overlap of the O2*s* and Y4*p* states increases.

The molecular vibrational spectra of complexes **I** and **II** are depicted in Fig. 3. The vibrations of structural subunits (complex ions) as a whole in **I** give rise to bands at 231, 279, and 309 cm^{-1}; in the case of **II**, these frequencies are lower: 100, 156, and 230 cm^{-1}. This is attributable to the large mass of $[YH\{N(CH_2PO_3)_3\}_2]^{8-}$ anion and low force constant of its ionic bond with the outer coordination sphere. In compound **I**, the mass of the [Y{NTP}] coordination sphere is probably lower and the bond between structural units is stronger, as indicated by the lack of water solubility of **I**; this bond might be covalent. The 480 and 550 cm^{-1} bands in the IR and Raman spectra of compound **I** refer to the δ(O–Y) modes; In structure **II**, vibrations of the coordination sphere produce a broad band at 500–640 cm^{-1}. The asymmetry of the Y CP in both structures is manifested as the absence of alternative selection of these vibrational modes. The 725, 760, 812, 856, 880, and 910 cm^{-1} modes refer to the N–C–P vibrations of ligand molecules. The ν(P–O) modes in complexes **I** and **II** give rise to bands at 943, 1002, 1073, 1128, and 1173 cm^{-1}, which do not

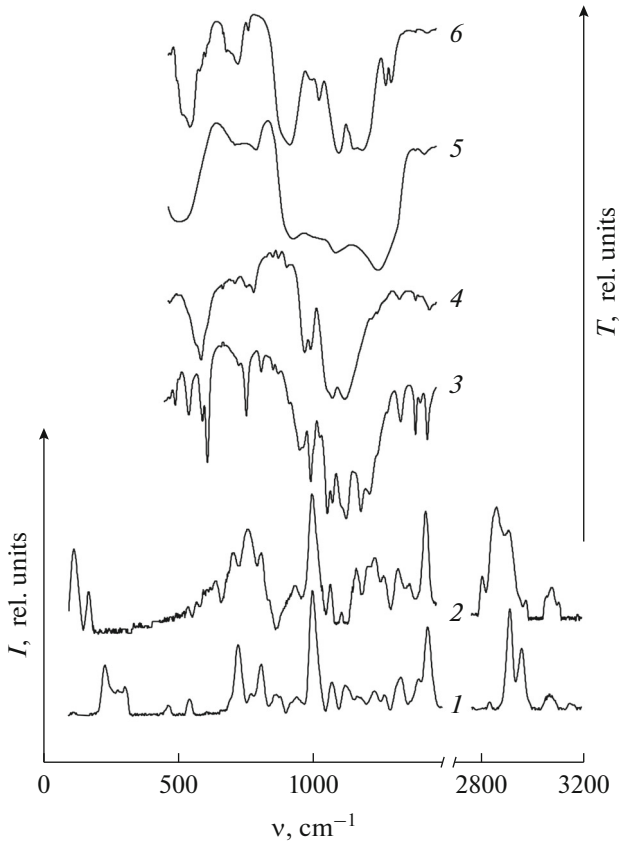

Fig. 3. Raman spectra (intensity *I* versus wave number ν) of complexes (*1*) **I** and (*2*) **II**; IR spectra (transmittance *T* versus wave number ν) of complexes (*3*) **I** and (*4*) **II** and the products of thermal decomposition under argon of complexes (*5*) **I** and (*6*) **II**.

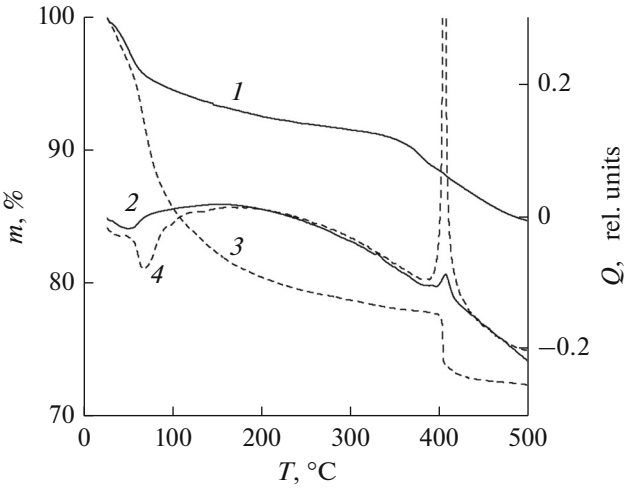

Fig. 4. Thermogravigrams of (*1* and *2*) **I** and (*3* and *4*) **II** under argon. Sample weight *m* (*1* and *3*) and heat *Q* (*2* and *4*) versus temperature *T*.

obey the alternative selection rules; this confirms the asymmetric conformation of the ligand molecule. The vibrational frequencies of the localized P–O π-bonds in compound **I** are 1234 and 1272 cm^{-1}, while in **II**, they are shifted to 1170 and 1225 cm^{-1}, which attests to a considerable electron density delocalization in the PO_3 groups. Also, the following bands are present (cm^{-1}): 1330 δ(*M*–O–H), 1430 δ(CH_2), 2770, 2830, 2890, 2950 ν(CH_2), 3050 ν(N^+–H).

Thermograms (Fig. 4) show that on heating of **I**, one H_2O molecule is eliminated in the 40–80°C range with a marked endothermic effect, while the other water molecule is split off in the broad range of 80–355°C. At 375–420°C, the N atom is eliminated with exothermic effect. The dehydration of **II** occurs in 65–95°C (–10H_2O) and 95–385°C (–5H_2O) ranges. The mass loss in the narrow range of 405–415°C corresponds to elimination of two CH_3NH_2 molecules with an explosive exothermic effect. Apparently, this attests to substantial mechanical strain in the chelate rings of **II**. The IR spectra of the thermal decomposition products of **I** and **II** (Fig. 3, *5* and *6*) show bands for the potassium phosphate glass $K_2O \cdot P_2O_5$ [54] (530, 730, 885–920, and 1090 cm^{-1}), potassium polymetaphosphate $(KPO_3)_n$ [55] (680, 760, 1100, 1150, 1270, and 1300 cm^{-1}), and yttrium orthophosphate YPO_4 [56, 57] (580, 997, and 1023 cm^{-1}).

Thus, the coordination compounds $[YH_3\{N(CH_2PO_3)_3\}] \cdot 2H_2O$ (**I**) and $K_8[YH\{N(CH_2PO_3)_3\}_2] \cdot 15H_2O$ (**II**) were synthesized, isolated, and studied for the first time. The structure of **II** was established by X-ray diffraction; the crystallographic details, the acid-base state, and the chemical function of nonequivalent ligand molecules were analyzed. The Y atom is seven-coordinate in the distorted trigonal antiprism geometry with an additional capping vertex above the base.

Presumably, compound **II** could be used as the precursor for the preparation of a uniform Y-containing adsorption layer on the steel surface followed by surface doping for increasing the heat resistance.

FUNDING

This work was performed as a part of the Government Assignment of the FASO of Russia (state registration number AAAA-A17-117022250040-0).

REFERENCES

1. *Comprehensive Coordination Chemistry*, Wilkinson G., Gillard, R.D., and McCleverty J.A., Eds., London: Pergamon, 1987, vol. 3.
2. *Koordinatsionnaya khimiya redkozemel'nykh elementov* (Coordination Chemistry of Rare Earth Elements), Spitsyn, V.I. and Martynenko, L.A., Eds., Moscow: MGU, 1979.

3. *Comprehensive Coordination Chemistry II*, McCleverty, J.A. and Meyer T.J., Eds., Elsevier, 2003, vol. 3.
4. Rösch, F., Herzog, H., Plag, C., et al., *Eur. J. Nucl. Med.*, 1996, vol. 23, no. 8, p. 958. doi 10.1007/BF01084371
5. Djokić, D.Dj., Jankovic′, D.Lj., and Nikolić, N.S. *Bioorg. Med. Chem.*, 2008, vol. 16, p. 4457. doi 10.1016/j.bmc.2008.02.062
6. Pillis, M.F. and Ramanathan, L.V., *Surf. Engineering*, 2006, vol. 22, no. 2, p. 129. doi 10.1179/174329406X98412
7. McGurty, J.A., US Patent 4385934.
8. Wegener, T. and Klein, F., Litnovsky, A., et al., *Nucl. Mater. Energy*, 2016, vol. 9, p. 394. doi 10.1016/j.nme.2016.07.011
9. Prajitno, D.H., Soepriyanto, S., Basuki, E.A., and Wiryolukito, S., *J. Mater. Sci. Engineering*, 2015, vol. 5, nos. 3–4, p. 154. doi 10.17265/2161-6213/2015.3-4.007
10. Grabke, H.J., *Surf. Interf. Anal.*, 2000, vol. 30, no. 1, p. 112. doi 10.1002/1096-9918(200008)30:1<112::AID-SIA777>3.0.CO;2-G
11. Wang, W., Wu, E., Liu, S., et al., *Mater. Sci. Technol.*, 2016, vol. 33, no. 1, p. 104. doi 10.1179/1743284715Y.0000000143
12. Patnaik, P., *Handbook of Inorganic Chemicals*, McGraw-Hill, 2002.
13. Gromov, V.E., Sosnin, K.V., Ivanov, Yu.F., et al., *Mater. Electron. Engineering*, 2015, vol. 2, no. 3, p. 1. doi 10.11605/mee-2-3
14. Sosnin, K.V., Ivanov, Yu.F., and Gromov, V.E., et al, *Metallurgist*, 2016, vol. 59, nos. 9–10, p. 829. doi 10.1007/s11015-016-0180-3
15. Wu, A., Liu, Q., and Qin, S., *J. Rare Earths*, 2011, vol. 29, no. 10, p. 1004. doi 10.1016/S1002-0721(10)60586-8
16. Pérez, F.J., Cristóbal, J., Hierro, M.P., et al., *Surf. Coat. Technol.*, 2000, vol. 126, p. 116. doi 10.1016/S0257-8972(99)00666-0
17. Han, B., Gu, D., Yang, Y., et al., *Int. J. Electrochem. Sci.*, 2017, vol. 12, p. 374. doi 10.20964/2017.01.53
18. Soleimannejad, J., Aghabozorg, H., Nakhjavan, B., et al., *Acta Crystallogr., Sect. E: Struct. Rep. Online*, 2007, vol. 63, p. m3170. doi 10.1107/S1600536807060047
19. Lv, Y.-K. and Gan, L.-H., Xu, L., et al., *Acta Crystallogr. Sect. E: Struct. Rep. Online*, 2011, vol. 67, p. m837. doi 10.1107/S1600536811019209
20. Zhang, C.-Y., Gao, Q., Cui, Y., and Xie, Y.-B., *Acta Crystallogr., Sect. E: Struct. Rep. Online*, 2008, vol. 64, p. m1631. doi 10.1107/S1600536808039421
21. Wharmby, M.T., Miller, S.R., Groves, J.A., et al., *Dalton Trans.*, 2010, vol. 39, p. 6389. doi 10.1039/c0dt00233j
22. Firmino, A.D.G., Mendes, R.F., Antunes, M.M., et al., *Inorg. Chem.*, 2017, vol. 56, p. 1193. doi 10.1021/acs.inorgchem.6b02199
23. Cabeza, A., Ouyang, X., Sharma, C.V.K., et al., *Inorg. Chem.*, 2002, vol. 41, p. 2325. doi 10.1021/ic0110373
24. Demadis, K.D., Katarachia, S.D., and Koutmos, M., *Inorg. Chem. Commun.*, 2005, vol. 8, p. 254. doi 10.1016/j.inoche.2004.12.019
25. Somov, N.V. and Chausov, F.F., *Cryst. Rep.*, 2014, vol. 59, no. 1, p. 66. doi 10.1134/S1063774513050118
26. Somov, N.V. and Chausov, F.F., *Cryst. Rep.*, 2015, vol. 60, no. 2, p. 210. doi 10.1134/S1063774515010228
27. Somov, N.V., Chausov, F.F., Zakirova, R.M., and Fedotova, I.V., *Russ. J. Coord. Chem.*, 2015, vol. 41, no. 12, p. 798. doi 10.1134/S1070328415110081
28. Somov, N.V., Chausov, F.F., Zakirova, R.M., and Fedotova, I.V., *Cryst. Rep.*, 2016, vol. 61, no. 2, p. 216. doi 10.1134/S1063774516020243
29. Somov, N.V. and Chausov, F.F., *Cryst. Rep.*, 2016, vol. 61, p. 39. doi 10.1134/S1063774516010235
30. Bazaga-García, M., Angeli, G.K., Papathanasiou, K.E., et al., *Inorg. Chem.*, 2016, vol. 55, p. 7414. doi 10.1021/acs.inorgchem.6b00570
31. Somov, N.V., Chausov, F.F., Zakirova, R.M., et al., *Russ. J. Coord. Chem.*, 2017, vol. 43, no. 12, p. 864. doi 10.1134/S1070328417120090
32. Somov, N.V., Chausov, F.F., Zakirova, R.M., et al., *Russ. J. Coord. Chem.*, 2017, vol. 43, no. 6, p. 373. doi 10.1134/S1070328417060082
33. Somov, N.V., Chausov, F.F., Zakirova, R.M., et al., *Cryst. Rep.*, 2017, vol. 62, no. 6, p. 857. doi 10.1134/S1063774517050224
34. Chausov, F.F., Somov, N.V., Naimushina, E.A., and Shabanova, I.N., *Bull. Russ. Acad. Sci.: Physics*, 2017, vol. 81, no. 3, p. 285. doi 10.3103/S106287381703007
35. Somov, N.V., Chausov, F.F., Lomova, N.V., et al., *Russ. J. Coord. Chem.*, 2017, vol. 43, no. 9, p. 583. doi 10.1134/S1070328417090093
36. Chausov, F.F., Somov, N.V., Zakirova, R.M., et al., *Bull. Russ. Acad. Sci.: Physics*, 2017, vol. 81, no. 3, p. 365. doi 10.3103/S106287381703008X
37. Chausov, F.F., Somov, N.V., Naimushina, E.A., et al., *Bull. Russ. Acad. Sci.: Physics*, 2016, vol. 80, no. 11, p. 1310. 10.3103/S1062873816110174
38. Sawada, K., Kuribayashi, M., Suzuki, T., and Miyamoto, H., *J. Solution Chem.*, 1991, vol. 20, no. 8, p. 829. doi 10.1007/BF00675114
39. Clark, R.C. and Reid, J.S., *Acta Crystallogr. Sect. A: Found. Crystallogr.*, 1995, vol. 51, p. 887. doi 10.1107/S0108767395007367
40. CrysAlisPro 1.171.38.41, Rigaku Oxford Diffraction, 2015.
41. Sheldrick, G.M., *Acta Crystallogr., Sect. A: Found. Crystallogr.*, 2008, vol. 64, p. 112. doi 10.1107/S0108767307043930
42. Farrugia, L.J., *J. Appl. Crystallogr.*, 1999, vol. 32, p. 837. doi 10.1107/S0021889899006020
43. Momma, K. and Izumi, F., *J. Appl. Crystallogr.*, 2011, vol. 44, p. 1272. doi 10.1107/S0021889811038970
44. Trapeznikov, V.A., Shabanova, I.N., Kholzakov, A.V., and Ponomaryov, A.G., *Relat. Phenom.*, 2004, vol. 137, p. 383. doi 10.1016/j.elspec.2004.02.115
45. Shirley, D.A., *Phys. Rev.*, 1972, vol. 55, p. 4709. doi 10.1103/PhysRevB.5.4709
46. Wojdyr, M., *J. Appl. Crystallogr.*, 2010, vol. 43, p. 1126. doi 10.1107/S0021889810030499
47. Cordero, B., Gómez, V., Platero-Prats, A.E., et al., *Dalton Trans.*, 2008, p. 2832. doi 10.1039/b801115j

48. Chausov, F.F., Naimushina, E.A., Shabanova, I.N., and Reshetnikov, S.M., *Bull. Russ. Acad. Sci.: Physics*, 2015, vol. 79, no 6, p. 848. doi 10.7868/S036767651506006X

49. Stevens, J.S., Byard, S.J., Muryn, C.A., and Schroeder, S.L.M., *J. Phys. Chem. B*, 2010, vol. 114, p. 13961. doi 10.1021/jp106465u

50. Desimoni, E. and Brunetti, B., *Chemosensors*, 2015, vol. 3, p. 70. doi 10.3390/chemosensors3020070

51. Hendrickson, D.N., Hollander, J.M., and Jolly, W.L., *Inorg. Chem.*, 1969, vol. 8, p. 2642. doi 10.1021/ic50082a020

52. Badrinarayanan, S., Sinha, S., and Mandale, A.B., *J. Electron Spectrosc. Related Phenom.*, 1989, vol. 49, p. 303. doi 10.1016/0368-2048(89)85018-2

53. Kawamura, M., Abe, Y., Yanagisawa, H., and Sasaki, K., *Thin Solid Films*, 1996, vol. 287, p. 115. doi 10.1016/S0040-6090(96)08749-4

54. de Andrade, J.S., Pinheiro, A.G., Vasconcelos, I.F., et al., *J. Phys.: Condens. Matter*, 1999, vol. 11, p. 4451. doi 10.1088/0953-8984/11/22/315

55. Corbridge, D.E.C. and Lowe, E.J., *J. Chem. Soc.*, 1954, p. 493. doi 10.1039/JR9540000493

56. Liu, Q., Su, Y., Yu, H., and Han, W., *J. Rare Earths*, 2008, vol. 26, no. 4, p. 495. doi 10.1016/S1002-0721(08)60125-8

57. Richman, I., *J. Optical Soc. Am.*, 1966, vol. 56, no. 11, p. 1589. doi 10.1364/JOSA.56.001589

Translated by Z. Svitanko